

\mathcal{PT} -symmetric interference transistor

Alexander A. Gorbatsevich^{1,2,*}, Gennadiy Ya. Krasnikov², and Nikolay M. Shubin^{1,2,3}

¹P.N. Lebedev Physical Institute of the Russian Academy of Sciences, Division of solid state physics, Moscow, 119991, Russia.

²JSC Molecular Electronics Research Institute, Zelenograd, Moscow, 124460, Russia.

³National Research University of Electronic Technology, Department of quantum physics and nanoelectronics, Zelenograd, Moscow, 124498, Russia.

*aagor137@mail.ru

February 21, 2022

Abstract

We present a model of the molecular transistor, operation of which is based on the interplay between two physical mechanisms, peculiar to open quantum systems that act in concert: \mathcal{PT} -symmetry breaking corresponding to coalescence of resonances at the exceptional point of the molecule, connected to the leads, and Fano-Feshbach antiresonance. This switching mechanism can be realised in particular in a special class of molecules with degenerate energy levels, i.e. diradicals, which possess mirror symmetry. At zero gate voltage infinitesimally small interaction of the molecule with the leads breaks the \mathcal{PT} -symmetry of the system that, however, can be restored by application of the gate voltage preserving the mirror symmetry. \mathcal{PT} -symmetry broken state at zero gate voltage with minimal transmission corresponds to the ‘off’ state while the \mathcal{PT} -symmetric state at non-zero gate voltage with maximum transmission – to the ‘on’ state. At zero gate voltage energy of the antiresonance coincides with exceptional point but the transmission variation mainly takes place due to the coalescence of resonances at the exceptional point. We construct a model of an all-electrical molecular switch based on such transistors acting as a conventional CMOS inverter and show that essentially lower power consumption and switching energy can be achieved, compared to the CMOS analogues.

1 Introduction

Implementation of molecules in integrated circuits (IC) offers great advantages due to extreme miniaturization and perfect reproducibility.[1, 2, 3] But despite long-term and intensive efforts since its origin in the early 70s,[4] molecular electronics (ME) has not yet presented any experimentally realized candidate to replace the silicon transistor as a ‘wheel-horse’ of the modern IC industry. High expectations were held and are still in place with graphene [5] and post graphene organic Dirac materials.[6] During past period ME mainly concentrated on the attempts to reproduce typical elements of silicon electronics.[7, 8, 9, 10, 11, 12] In the case of graphene and related materials this approach has been based on the efforts to develop band opening methods,[13] which, however, haven’t resulted yet in a new IC technology either. On the other hand, due to complex geometry and topology of molecular structures one could expect that the devices with working principles, different from the ordinary field-effect and bipolar transistors, could be designed.

Energy spectrum of a molecule manifests itself in transport phenomena by means of resonances. If the molecule possesses different carrier paths, destructive interference can result in formation of asymmetric Fano-Feshbach resonance,[14] which combines a resonance (transmission peak) and an antiresonance (transmission dip) nearby. Existence of the interference effect in transport through molecules, which is intensively discussed in the literature,[15, 16, 17, 18, 19] is now well established experimentally.[20, 21, 22, 23] In Ref. [24] quantum interference transistor (QIT) was described with the ‘off’ state corresponding to perfect interference destruction of both transmission and current. One of the main challenges in CMOS electronics is reduction of the operating voltage that doesn’t follow Moore’s law (ITRS 2.0). In Ref. [25] it was argued that the interference control of the carrier transport over different paths can substantially reduce the operating gate voltage, because the suppression

of the transmission function can be achieved at lower gate voltage compared with the one required to move the transmission function peak away from the distribution function window. However, antiresonances, which arise from the destructive quantum interference (DQI), are determined by the topology of the structure that includes different interfering carrier paths. Hence, variation of the on-site potential and/or intersite hopping can only shift the antiresonance in energy rather than destroy it, because interfering paths are retained under such variations. The voltage required to shift an antiresonance away from the operating energy region is determined by the carrier distribution in the leads on a scale no less than kT and, hence, is not small. Therefore, the proposed control of the transmission resonance by low voltages should rely on a mechanism more complex than multipath interference solely. For a logical gate to operate, its constituting elements (transistors) should undergo transitions between the ‘off’ and the ‘on’ states, with the latter state being even more important than the former one as it provides switching of the successive gate. The ‘on’/‘off’ ratio for the transistor conductance should be as high as possible to provide a reliable gate operation. However, this requirement is scarcely achievable in quantum interference transistors operating near the antiresonance because of the low transmission away from the antiresonance.[26] Hence, a quantum transistor is required, which possesses a combination of antiresonance and nearby resonance that is responsible for high conductance in the ‘on’ state.

In this paper we show that, indeed, the transmission probability of a special class of molecules can be controlled in a wide range by applying small gate voltages due to the interplay of two physical mechanisms: \mathcal{PT} -symmetry breaking, accompanied by the collapse of resonances[27] at the exceptional point (EP) of the molecule connected to the leads,[28, 29] and the shift of Fano-Feshbach resonance to the EP point. This special class consists of the molecules with degenerate energy levels, e.g. diradicals[30, 31, 32] (but not restricted to), which possess mirror symmetry.

2 Phenomenological model

Consider an open quantum system comprised of a molecule and contacts that possesses EP in a sense of Ref. [29]. At this EP two unity resonances coalesce and cancel each other making the transition to the ‘off’ state very sharp. An open quantum system should be spatially symmetric in order to possess EP. To take advantage of both DQI and coalescence of resonances at the EP one should consider a system with two resonances and one antiresonance. The transmission coefficient of an arbitrary two-terminal quantum system can be written in the compact form: [28, 29]

$$T(\omega) = \frac{|P(\omega)|^2}{|P(\omega)|^2 + |Q(\omega)|^2}. \quad (1)$$

Here $P(\omega)$ and $Q(\omega)$ are some functions of an energy ω . Real zeroes of function $P(\omega)$ correspond to transmission nodes (antiresonances), while real zeroes of function $Q(\omega)$ determine exact positions of perfect (unity) resonances on the energy axis.[28, 29] In the vicinity of the resonances and antiresonance $P(\omega)$ and $Q(\omega)$ can be expressed as:[29]

$$\begin{aligned} P(\omega) &= 2\Gamma B (\omega - \varepsilon_0) D_P, \\ Q(\omega) &= (\omega - \varepsilon_1^+) (\omega - \varepsilon_1^-) D_Q, \end{aligned} \quad (2)$$

where ε_0 and ε_1^\pm determine exact position of the transmission antiresonance and resonances, correspondingly, Γ is the imaginary part of the contact self-energy describing interaction of a molecule with the leads[33, 34] and B is some positive dimensionless coefficient. Factors D_P and D_Q take into account the contributions from the remote energy levels and can be estimated as $D_P \sim D_Q \sim \Delta^{N-2}$, where Δ is an average distance between the remote energy levels and N is the dimension of the molecular orbital Hilbert space. Phenomenologically, functions $P(\omega)$ and $Q(\omega)$ are defined up to an arbitrary common factor, hence, we can redefine the parameter $B \mapsto BD_P/D_Q$ and replace three phenomenological parameters B , D_P and D_Q by just B . Further we will use B as such generalized parameter.

Consider a model that possesses degenerate antiresonance and resonance levels in the symmetric phase, which can be distorted by an external perturbation described by parameter δ . Energies of the antiresonance ε_0 and resonances ε_1^\pm can be expressed as:

$$\begin{aligned} \varepsilon_0 &= x_0 \delta, \\ \varepsilon_1^\pm &= x_1 \delta \pm \sqrt{y^2 \delta^2 - z^2 \Gamma^2}. \end{aligned} \quad (3)$$

Here $x_{0,1}$, y and z are some dimensionless parameters depending on the structure of a particular system. Terms in Eq. (3), which are linear in δ , describe the shift of the (anti)resonance positions due to the external perturbation and non-analytical term (square root) in the expression for ε_1^\pm describes the coalescence of resonances phenomenon. Energy of the degenerate state (at $\delta = 0$) is set to the energy origin. If the external perturbation δ is high enough ($\delta > zy^{-1}\Gamma$), then the transmission has two unity peaks at $\omega = \varepsilon_1^\pm$, which coalesce at $\delta = zy^{-1}\Gamma$. The poorest transmission profile (i.e. the ‘off’ state) corresponds to $\delta = 0$. From Eqs. (1-3) one can see, that in this case there are two peaks at $\omega = \pm z\Gamma$ with

$$T_{peak}(\omega = \pm z\Gamma; \delta = 0) = \frac{B^2}{B^2 + z^2}, \quad (4)$$

separated by a zero dip at $\omega = 0$.

3 Microscopic model

The microscopic model of the system, transmission coefficient of which possesses the phenomenological properties described above, is as follows. There are two degenerate states $|1\rangle$ and $|2\rangle$ with the same energy ε . This system is attached symmetrically to two leads (left and right) in such a way that the mirror symmetry operation σ_{LR} , which maps the left lead into the right one and vice versa, is also an element of the symmetry group G of the bare Hamiltonian of the system, i.e. $\sigma_{LR} \in G$. Due to the degeneracy, there must be an irreducible representation of the symmetry group G acting on the subspace $\mathcal{H}_{12} = \text{Span}(|1\rangle, |2\rangle)$ of the total Hilbert space of states of the isolated system. Let us choose the basis in \mathcal{H}_{12} as the basis of a symmetric $|s\rangle$ and an anti-symmetric $|a\rangle$ states, which are the eigenstates of the reflection operator σ_{LR} : $\sigma_{LR}|s\rangle = |s\rangle$ and $\sigma_{LR}|a\rangle = -|a\rangle$. These states conserve their symmetry with introduction of the perturbation, which is invariant under σ_{LR} . The tunnelling matrix elements between the leads and the symmetric state are of the same sign, whereas, the tunnelling matrix elements between the leads and the anti-symmetric state are of opposite signs (see Fig. 1a). Therefore in this basis couplings to the leads can be written as

$$\begin{aligned} \mathbf{u}_L &= \sqrt{\Gamma} \begin{pmatrix} \gamma_s \\ \gamma_a \end{pmatrix}, \\ \mathbf{u}_R &= \sqrt{\Gamma} \begin{pmatrix} \gamma_s \\ -\gamma_a \end{pmatrix}. \end{aligned} \quad (5)$$

Here Γ governs the coupling strength and positive dimensionless parameters $0 \leq \gamma_{s,a} \leq 1$ describe relative couplings of symmetric and anti-symmetric states to the leads. Parameters $\gamma_{s,a}$ can be calculated, for example, as projections of the vector $\Gamma^{-1/2}\mathbf{u}_{L,R}^{site}$ onto $|s\rangle$ or $|a\rangle$ respectively, where $\mathbf{u}_{L,R}^{site}$ describes the coupling to the leads in the site (atomic orbitals) basis. If each lead is attached to only one site, then $\gamma_{s,a}$ is just a contribution of the state localized in the connection site to the symmetric or anti-symmetric state correspondingly (see Supplementary materials).

Application of the gate voltage introduces external perturbation that lowers the symmetry of the system, resulting in removal of the degeneracy. Suppose that the external perturbation lowers the symmetry of the system from the group G to its some non-trivial subgroup $H \subset G$, such that $\sigma_{LR} \in H$. This perturbation introduces detuning of the energy of symmetric and anti-symmetric states: $\varepsilon_{s,a}(\delta) = \varepsilon + k_{s,a}\delta$ with $\delta > 0$ and dimensionless parameters $-1 \leq k_{s,a} \leq 1$ accounting for the different influence of the perturbation on the energies of symmetric and anti-symmetric states (see Fig. 1a). So, the bare Hamiltonian of the system becomes following:

$$\hat{H}_0 = \begin{pmatrix} \varepsilon + k_s\delta & 0 \\ 0 & \varepsilon + k_a\delta \end{pmatrix} \quad (6)$$

Parameters $k_{s,a}$ can be estimated, for instance, from the perturbation theory (see Supplementary materials for details); note that $k_a \neq k_s$ as the considered perturbation removes the degeneracy. Assume that couplings (5) are not affected by this perturbation. In fact, Γ and $\gamma_{s,a}$ are some smooth functions of the perturbation strength, i.e. δ . However, taking this into account does not change the qualitative picture described below.

3.1 Transport properties

Tunnelling transmission coefficient through the states $|s\rangle$ and $|a\rangle$ (neglecting the contribution from remote states to the transport process) can be calculated by the standard formula:[33]

$$T = 4 \text{Tr} \left(\hat{\Gamma}_R \hat{G}^r \hat{\Gamma}_L \hat{G}^a \right), \quad (7)$$

where $\hat{G}^{r,a}$ is the retarded/advanced Green function and $\hat{\Gamma}_{L,R} = \mathbf{u}_{L,R} \mathbf{u}_{L,R}^\dagger$ [35] is the coupling matrix (imaginary part of corresponding contact self-energy) to the left or to the right lead. Here $\mathbf{u}_{L,R}$ are vectors, describing couplings of the states of the isolated system to the left/right lead. Traditional approach within the wide-band limit (neglecting real parts of the contact self-energy) leads to the following expression for the transmission:[29]

$$T = \frac{4 \left| \det \left(\omega \hat{I} - \hat{H}_0 \right) \right|^2 \left| \mathbf{u}_R^\dagger \left(\omega \hat{I} - \hat{H}_0 \right)^{-1} \mathbf{u}_L \right|^2}{\left| \det \left(\omega \hat{I} - \hat{H}_{eff} \right) \right|^2}, \quad (8)$$

where $\hat{H}_{eff} = \hat{H}_0 - i \mathbf{u}_L \mathbf{u}_L^\dagger - \mathbf{u}_R \mathbf{u}_R^\dagger$ is the Feshbach effective Hamiltonian. Following general formalism from Ref. [29], one can show that transmission (8) can be written in the form (1). For our microscopic model this can be easily checked using Eqs. (5) and (6). Indeed, the following identity holds true:

$$\begin{aligned} |Q|^2 &= \left| \det \left(\omega \hat{I} - \hat{H}_0 - i \mathbf{u}_L \mathbf{u}_L^\dagger + \mathbf{u}_R \mathbf{u}_R^\dagger \right) \right|^2 = \left| \det \left(\omega \hat{I} - \hat{H}_0 + i \mathbf{u}_L \mathbf{u}_L^\dagger + \mathbf{u}_R \mathbf{u}_R^\dagger \right) \right|^2 \\ &\quad - 4 \left| \det \left(\omega \hat{I} - \hat{H}_0 \right) \right|^2 \left| \mathbf{u}_R^\dagger \left(\omega \hat{I} - \hat{H}_0 \right)^{-1} \mathbf{u}_L \right|^2 = [4\Gamma^2 \gamma_a^2 \gamma_s^2 + (\omega - \varepsilon - k_s \delta)(\omega - \varepsilon - k_a \delta)]^2. \end{aligned} \quad (9)$$

Hence, from Eq. (9) we see that within the wide-band limit, the transmission of our system can be written in the form (1) with

$$\begin{aligned} P(\omega) &= 2 \det \left(\omega \hat{I} - \hat{H}_0 \right) \times \mathbf{u}_L^\dagger \left(\omega \hat{I} - \hat{H}_0 \right)^{-1} \mathbf{u}_R, \\ Q(\omega) &= \det \left(\omega \hat{I} - \hat{H}_{aux} \right). \end{aligned} \quad (10)$$

Here

$$\hat{H}_{aux} = \hat{H}_0 + i \mathbf{u}_L \mathbf{u}_L^\dagger - i \mathbf{u}_R \mathbf{u}_R^\dagger = \begin{pmatrix} \varepsilon + k_s \delta & 2i\Gamma \gamma_s \gamma_a \\ 2i\Gamma \gamma_s \gamma_a & \varepsilon + k_a \delta \end{pmatrix} \quad (11)$$

is the non-Hermitian auxiliary Hamiltonian with its real eigenvalues corresponding to energies of perfect transmission,[29] and \hat{I} is the 2×2 identity matrix. Hamiltonian \hat{H}_{aux} is \mathcal{PT} -symmetric, where $\mathcal{P} = \sigma_{LR}$ denotes to the mirror reflection and \mathcal{T} is the time reversal operator (complex conjugation). Indeed, one can easily check that operator $\mathcal{PT} \hat{H}_{aux} \mathcal{PT}$ acts on any vector $\mathbf{v} \in \mathbb{C}^2$ in the same way as operator \hat{H}_{aux} . Thus, \hat{H}_{aux} is \mathcal{PT} -symmetric.[36] Therefore, it can possess real eigenvalues, which correspond to perfect transmission peaks, and for certain parameters they can coalesce and the \mathcal{PT} -symmetry of the Hamiltonian \hat{H}_{aux} will be broken, leading to coalescence of perfect resonances into one peak with amplitude lower than 1. Moreover, such resonance coalescence is accompanied by symmetry breaking of electron occupation at the energy corresponding to the transmission peak (see Appendix 5 for details).

Using Eqs. (5-11), the transmission coefficient can be written as:

$$T(\omega) = \frac{4\Gamma^2 \left[(k_a \gamma_s^2 - k_s \gamma_a^2) \delta - (\gamma_s^2 - \gamma_a^2) (\omega - \varepsilon) \right]^2}{4\Gamma^2 \left[(k_a \gamma_s^2 - k_s \gamma_a^2) \delta - (\gamma_s^2 - \gamma_a^2) (\omega - \varepsilon) \right]^2 + \left\{ \left[\omega - \varepsilon - \frac{1}{2} \delta (k_a + k_s) \right]^2 + 4\gamma_s^2 \gamma_a^2 \Gamma^2 - \delta^2 \frac{(k_a - k_s)^2}{4} \right\}^2}. \quad (12)$$

From this formula one can see that for a sufficiently large detuning δ there are two unity peaks of transmission (zeros of Q , i.e. eigenvalues of \hat{H}_{aux}) at $\omega = \varepsilon + \frac{1}{2} \delta (k_a + k_s) \pm \sqrt{\frac{1}{4} \delta^2 (k_a - k_s)^2 - 4\gamma_s^2 \gamma_a^2 \Gamma^2}$. Decreasing the detuning one can achieve the coalescence of resonances at $\delta = 4\gamma_s \gamma_a \Gamma |k_a - k_s|^{-1}$, which correspond to the EP of \hat{H}_{aux} .

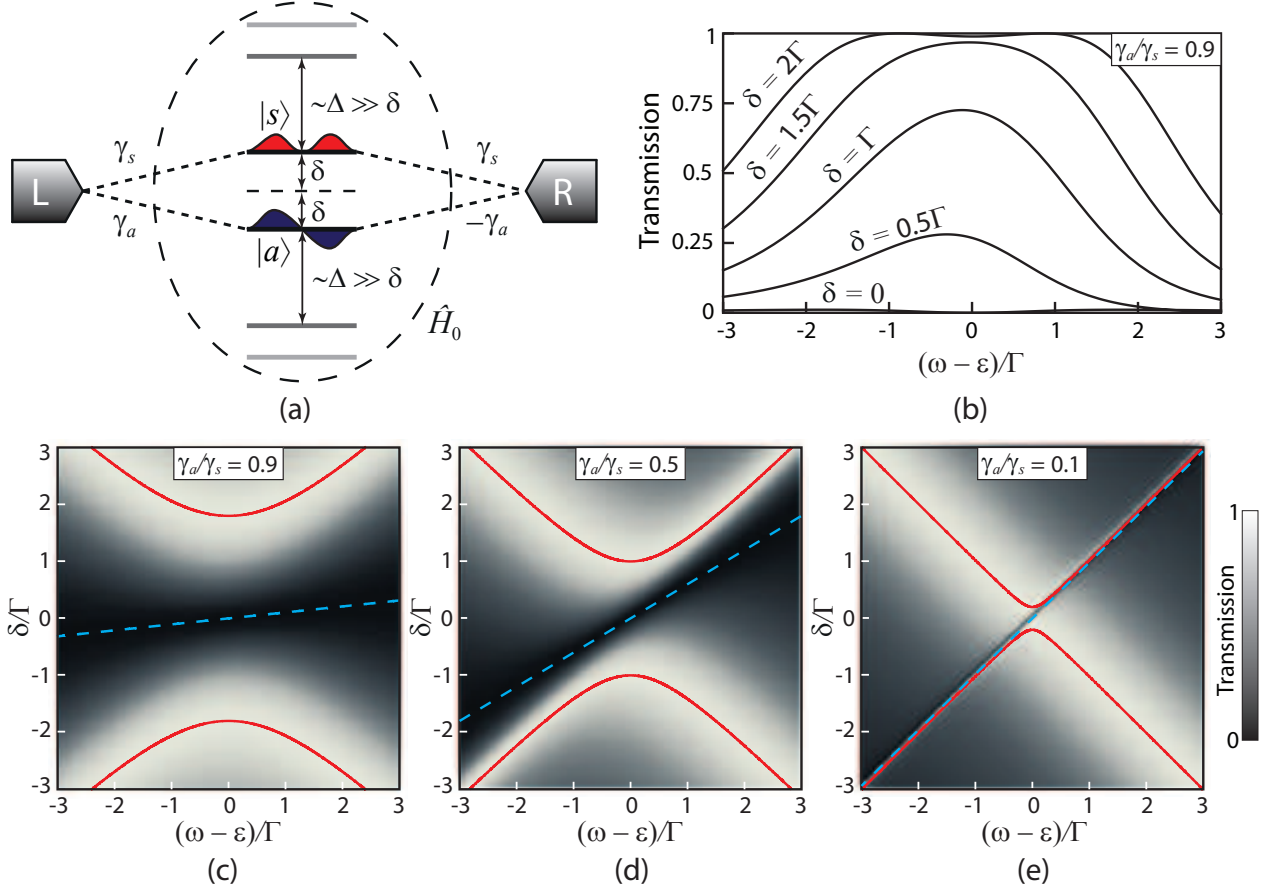


Figure 1: Microscopic model and its transmission coefficient. (a) Schematic view of the microscopic model of the molecular system depicting symmetric $|s\rangle$ and anti-symmetric $|a\rangle$ states connected to the leads by couplings (5). Γ is set as energy unit and $k_a = -k_s = 1$ for convenience. Evolution of the transmission coefficient profile with variation of δ (γ_s is set to 1 and $k_a = -k_s = 1$) for (b) some discrete values of δ for $\gamma_a = 0.9$, and (c-e) in the form of density plots for (c) $\gamma_a = 1$, (d) $\gamma_a = 0.5$ and (e) $\gamma_a = 0.1$. Red solid lines indicate the position of perfect resonances and dashed cyan – zeros of the transmission.

Further decreasing δ results in further lowering of the transmission coefficient peak. There is also a zero-valued antiresonance (zero of P) at $\omega = \epsilon + \delta(k_a\gamma_s^2 - k_s\gamma_a^2)/(\gamma_s^2 - \gamma_a^2)$, which additionally lowers the transmission with decreasing δ . One can see that, moving the energy origin to ϵ , Eq. (12) takes the phenomenological form described by Eqs. (1-3) with the following phenomenological parameters:

$$B = |\gamma_s^2 - \gamma_a^2| \quad x_0 = \frac{k_a\gamma_s^2 - k_s\gamma_a^2}{\gamma_s^2 - \gamma_a^2}, \quad x_1 = \frac{k_a + k_s}{2}, \quad y = \frac{|k_a - k_s|}{2}, \quad z = 2\gamma_s\gamma_a. \quad (13)$$

Thus, according to Eq. (4) one can see that the poorest transmission peaks (at $\delta = 0$) are

$$T_{peak}(\omega = \epsilon \pm 2\gamma_s\gamma_a\Gamma; \delta = 0) = \frac{(\gamma_s^2 - \gamma_a^2)^2}{(\gamma_s^2 + \gamma_a^2)^2}. \quad (14)$$

From (13) we see that there is a limiting case $\gamma_s/\gamma_a \rightarrow 1$ that results in $B \rightarrow 0$ and $x_0 \rightarrow \infty$, while the product $Bx_0 \rightarrow \gamma_{s,a}^2(k_a - k_s)$ remains finite. In this case complete opaqueness, i.e. $T \equiv 0$, can be obtained for $\delta = 0$. In practice, however, the transmission never vanishes because of the transport through remote energy levels, which are not taken into account in this model. Evolution of the transmission coefficient profile (12) with variation of δ for different ratios of the parameters γ_s and γ_a is illustrated in Fig. 1c-e.

4 Quantum interference inverters based on \mathcal{PT} -symmetric interference transistors

Consider a quantum analogue of CMOS inverter consisting of two quantum switches, connected between one common output lead and two reference voltage sources with voltages V_{ref1} and V_{ref2} , respectively. Input signal V_{in} is applied to the common gate of these switches, which is galvanically isolated from the system. Figure 2 depicts two examples of such quantum interference inverters. For a high-resistance load we can implicitly evaluate the voltage transfer characteristic $V_{out}(V_{in})$ of this inverter and estimate its maximum negative gain, which is achieved at $V_{in} = \frac{1}{2}(V_{ref1} + V_{ref2})$ due to the symmetry. To do so, the transmission coefficients between the leads T_{1out} , T_{2out} and T_{12} should be determined first. Reference voltages V_{ref1} and V_{ref2} (assume $V_{ref1} < V_{ref2}$) are given by some external ideal voltage sources, i.e. we treat them as constants. As the input lead is isolated from the system, the voltage V_{in} influences only transmission coefficients. For high-resistance loads the output voltage V_{out} is derived from the condition $I_{out} = 0$, where I_{out} is the total current through the output lead, which is composed of the currents from the first and the second reference voltage leads (with appropriate sign).

Let us consider an inverter composed of two identical quantum switches (\mathcal{PT} -symmetric interference transistors). Assuming that resonance width is sufficiently small, we can approximate condition $I_{out} = 0$ as follows:

$$\begin{aligned} [f(\varepsilon_1 - eV_{out}) - f(\varepsilon_1 - eV_{ref1})] \times \frac{(\gamma_s^2 + \gamma_a^2) [\delta_1^2 (k_a - k_s)^2 + 4\Gamma^2 (\gamma_a^2 - \gamma_s^2)^2]}{\delta_1^2 (k_a - k_s)^2 + 4\Gamma^2 (\gamma_s^2 + \gamma_a^2)^2} \\ = [f(\varepsilon_2 - eV_{ref2}) - f(\varepsilon_2 - eV_{out})] \times \frac{(\gamma_s^2 + \gamma_a^2) [\delta_2^2 (k_a - k_s)^2 + 4\Gamma^2 (\gamma_a^2 - \gamma_s^2)^2]}{\delta_2^2 (k_a - k_s)^2 + 4\Gamma^2 (\gamma_s^2 + \gamma_a^2)^2}. \end{aligned} \quad (15)$$

Here subscripts 1 and 2 correspond to the first and to the second quantum switches. Energies $\varepsilon_{1,2}$ are the energies of degenerate states in the first and in the second system respectively. Assume that they are adjusted to $\varepsilon_{1,2} = eV_{ref1,2}$, i.e. to the biased Fermi level of each reference lead. The applied input voltage influences parameters $\delta_{1,2}$ of the switches. The following model dependence of $\delta_{1,2}$ on the input voltage V_{in} provides a symmetrical transition from the ‘on’-mode to the ‘off’-mode of each quantum switch as V_{in} varies in the interval $[V_{ref1}, V_{ref2}]$:

$$\delta_{1,2} = \alpha e (V_{in} - V_{ref1,2}), \quad (16)$$

where $0 < \alpha < 1$ is an electrostatic lever arm of the input lead (common gate). One can substitute Eq. (16) into Eq. (15) and derive the implicit dependence $V_{out} = V_{out}(V_{in})$, which then can be used to get an expression for the maximum gain:

$$\begin{aligned} G_{max} = G \left(V_{in} = \frac{V_{ref1} + V_{ref2}}{2} \right) \\ = \sinh \frac{e\Delta V}{2kT} \times \frac{256\alpha^2 \Gamma^2 \gamma_a^2 \gamma_s^2 (k_a - k_s)^2 kT e \Delta V}{\left[16\Gamma^2 (\gamma_s^2 - \gamma_a^2)^2 + \alpha^2 (k_a - k_s)^2 e^2 \Delta V^2 \right] \left[16\Gamma^2 (\gamma_s^2 + \gamma_a^2)^2 + \alpha^2 (k_a - k_s)^2 e^2 \Delta V^2 \right]}. \end{aligned} \quad (17)$$

Here $\Delta V = V_{ref2} - V_{ref1}$ is fixed by the external supply voltage. In the saturation regime ($e\Delta V \gg kT$) the maximum value of G grows exponentially with ΔV due to the factor $\sinh \frac{e\Delta V}{2kT}$. For $e\Delta V \lesssim kT$ (in the ohmic regime) it becomes independent of the temperature and we can estimate the minimum difference of the reference voltages (supply voltage) ΔV_{crit} needed to make the inverter operate, i.e. which provides $G_{max} = 1$:

$$\Delta V_{crit} \approx \frac{4\Gamma}{e\alpha |k_a - k_s|} \sqrt{4\gamma_a^2 \gamma_s^2 - \gamma_s^4 - \gamma_a^4 - 2\gamma_a \gamma_s \sqrt{5\gamma_a^2 \gamma_s^2 - 2\gamma_s^4 - 2\gamma_a^4}} \sim |\gamma_s - \gamma_a| \text{ as } \frac{\gamma_a}{\gamma_s} \rightarrow 1. \quad (18)$$

From Eq. (18) one can see that ΔV_{crit} can become infinitesimal as $\gamma_a/\gamma_s \rightarrow 1$. On the other hand, however, G_{max} remains bounded in the ohmic regime even if $\gamma_a/\gamma_s \rightarrow 1$. From the analysis of Eq. (17) one can conclude that for $\Delta V = 4 \frac{\Gamma}{e\alpha |k_a - k_s|} \sqrt{|\gamma_s^4 - \gamma_a^4|}$ the gain G_{max} reaches its maximum: $2(\gamma_s/\gamma_a)^2$ for $\gamma_s < \gamma_a$ or $2(\gamma_a/\gamma_s)^2$ for $\gamma_s > \gamma_a$. Hence, the steepest negative gain of the voltage transfer characteristic is limited to -2 . Nevertheless, it is suitable for operation of the inverter.

4.1 Model examples of real molecular structures

Possible candidates for a physical realization of the proposed quantum switch are molecules with degenerate states, e.g. diradicals, [30] which are already known for providing transmission antiresonances. [31] Moreover, linkers can stabilize diradical character of such molecules. [37] Hence, we can expect that connection of certain contacts to them will not destroy the degeneracy of the states, but rather stabilize it. Diradicals can be classified into two types: disjoint and non-disjoint depending on how their non-bonding orbitals intersect (i.e. whether they have common atomic orbitals or not). It was shown that simple starring procedure can distinguish between these two types. [38, 39] Disjoint diradicals seem to be the most appropriate candidate for our quantum switch. Indeed, applying contacts to atoms comprising different degenerate orbitals means that symmetric and antisymmetric combinations of these orbitals will be connected to the leads by equivalent coupling strength, i.e. parameters γ_s and γ_a [introduced in Eq. (5)] in this case can be made equal (at least within the nearest neighbour tight-binding approximation). As was highlighted above, according to Eq. (14) this leads to zero conductance in the ‘off’ state.

Operation principle of quantum interference inverter requires that one switch must be in the ‘on’ state and another in the ‘off’ state. There are two possible ways of dealing with this task. First of all, one can choose two different quantum systems (molecules) to make two quantum switches that is similar to the conventional CMOS, where there are two different types of transistors: n-channel MOS and p-channel MOS. This approach requires a technology of synthesis of two different molecules with strictly given parameters. On the other hand, we can use the same quantum system (molecule) to create both switches, but influence their spectrum in different ways by additional gates. This method needs only one type of molecule to be synthesised, but the introduction of additional gates results in some complication of the conventional technological process. In the following subsections we consider some schematic examples of quantum inverters with the same molecules in both switches. Different energies of the on-site atomic states are assumed to be achieved by a certain configuration of additional gates.

4.1.1 Model of non-disjoint diradical

The first example structure we consider is a model of the trimethylenemethane molecule, which is a non-disjoint diradical. [31] Schematically the quantum inverter structure composed of two such four-atomic (carbon skeleton) molecules is shown in Fig. 2a. Presented schematic model corresponds to a tight-binding Hückel structure of one of the resonance configurations of the trimethylenemethane, which is stabilized as it coincides in symmetry with the leads couplings. Hence, hopping integral τ is assumed to be greater than τ_1 as it corresponds to a higher bond order. The transmission coefficient, phenomenological, and microscopical parameters of such switches are presented in the Supplementary material.

We apply the reference voltages as follows: $V_{ref1} = 0$ and $V_{ref2} = V_0$ is the supply voltage. The range of the input voltage, thus, is $0 \leq V_{in} \leq V_0$. Applied input potential changes only some on-site energies of the system (in the shaded region in Fig. 2a). We take this into account in the following form:

$$\varepsilon_0^{1,2} = \varepsilon_{1,2} + \alpha e (V_{in} - V_{ref1,2}). \quad (19)$$

The electrostatic influence of the reference and output leads can also be taken into account in a way similar to (19). It can be shown that this influence only distorts the voltage transfer characteristic and taking it into account is not obligatory to illustrate the operation principles of the quantum interference inverters.

Consider the following example: $\varepsilon_1 = eV_{ref1} = 0$, $\varepsilon_2 = eV_{ref2} = eV_0$, $\alpha = 0.5$, $\tau_1 = 1\text{eV}$, $\tau = 2\text{eV}$ and $\Gamma = 1\text{meV}$. Energies are measured from the Fermi level of the first reference lead. Figure 3a shows voltage transfer characteristics of the inverter for $V_0 = 5\text{mV}$ and Fig. 3b – for $V_0 = 10\text{mV}$ (by dot-dashed lines in both cases). In the latter case the voltage transfer characteristic is obviously better because of higher negative gain achieved.

4.1.2 Model of disjoint diradical

Another example we consider is a model of the divinylcyclobutadiene molecule, which is a disjoint diradical. [31] Schematically the quantum inverter structure composed of two such molecules is shown in Fig. 2b. Presented model corresponds to a simple tight-binding Hückel structure of the divinylcyclobutadiene molecule with all bonds treated as equal, providing equal tunnelling matrix elements τ between p-orbitals of carbon atoms. The transmission coefficient, phenomenological, and microscopical parameters of such switches are presented in the Supplementary material.

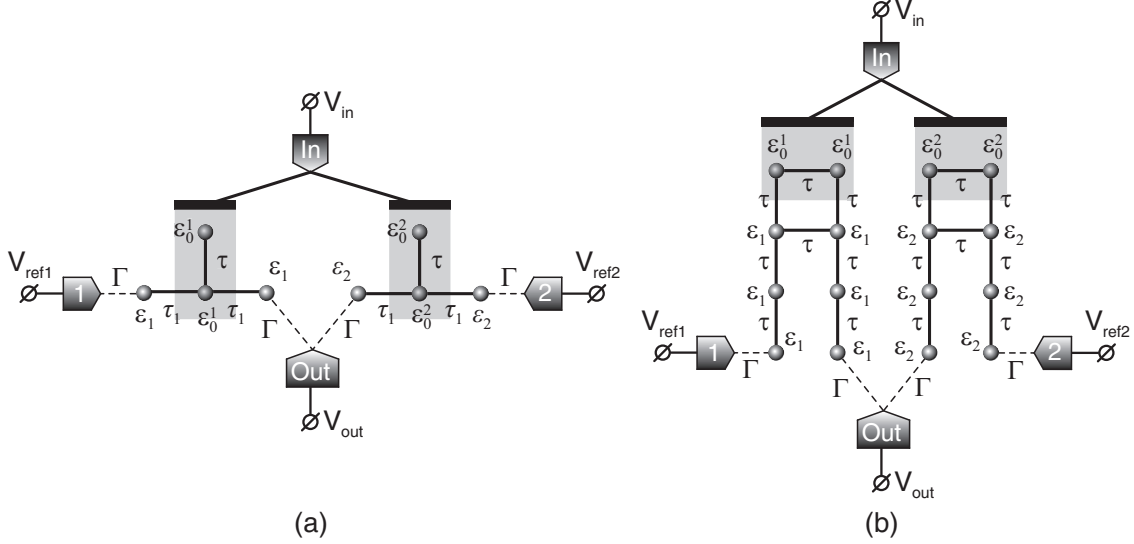


Figure 2: Model structures of quantum interference inverter, composed of two quantum switches based on (a) non-disjoint diradicals and (b) disjoint diradicals. Molecules are shown in the form of their Hückel theory tight-binding graphs. Shaded regions indicate the sites, which are electrostatically affected by the input gate.

We assume that the applied input voltage changes only on-site energies in the shaded region in Fig. 2b, which is taken into account similarly to Eq. (19). Figure 3a shows voltage transfer characteristics of this inverter for $V_0 = 5\text{mV}$ and Fig. 3b – for $V_0 = 10\text{mV}$ (by solid lines in both cases) for the following parameters: $\varepsilon_1 = eV_{ref1} = 0$, $\varepsilon_2 = eV_{ref2} = eV_0$, $\alpha = 0.5$, $\tau = 1\text{eV}$ and $\Gamma = 1\text{meV}$.

For higher supply voltage transfer characteristic of the inverter based on the disjoint diradical switches (solid lines in Fig 3b) show higher maximum absolute value of the gain rather than for the inverter based on the non-disjoint diradical switches (dot-dashed lines in Fig 3b). This is expectable as disjoint diradicals provide $\gamma_s/\gamma_a = 1$ and, thus, the ‘off’-state current of such switch becomes smaller (it differs from zero only due to the presence of the ‘background’ transmission arising from remote resonance peaks). However, for smaller supply voltage (Fig. 3a), this ‘background’ component may become high enough to cancel out the key benefit of the disjoint diradical ($\gamma_s/\gamma_a = 1$). Moreover, for lower supply voltages, the range of possible variation of δ becomes smaller and, due to the non-linearity of energy shifts for disjoint diradicals (i.e. $k_{a,s}$ become functions of δ), the sensitivity to the gate voltage decreases compared to non-disjoint diradicals. In this case the transfer characteristic of a non-disjoint diradical turns out to be more suitable (Fig. 3a).

5 Discussion

We have shown that utilizing the degeneracy of the quantum system spectrum, one can construct the quantum switch operating at infinitesimal supply voltage even at room temperature. Moreover, we propose that a special class of widely studied organic molecules – diradicals can pretend to make a physical realization of such switches. Thus, this might be a way to dramatically lower the supply voltage, which now cannot be made lower than 0.5-1V[40] for the conventional silicon electronic devices, even for promising tunnel field-effect transistors (FET).[41] Advance technology of FETs with carbon nanotube (CNT) channel[42] also provides a variety of advantages over the bulk Si electronics,[43, 10] but sufficient reduction of the supply voltage is not among them.

However, the question about the noise influence comes up, if we consider low supply voltages and especially sub- kT/e voltages. Strictly speaking, noise in quantum systems is not distinguished into thermal and shot, it is always a superposition of both and it can be described by a closed expression.[44] Nevertheless, it is illustrative to discuss these contributions independently. Shot noise spectral power is proportional to the current through the system and, thus, it becomes negligible as the voltages and, correspondingly, the currents are scaled down. On the other hand, at finite (room) temperature thermal noise can influence the transport dramatically. Thus, thermal noise is one of the limiting factors of lowering the supply voltage.[40]

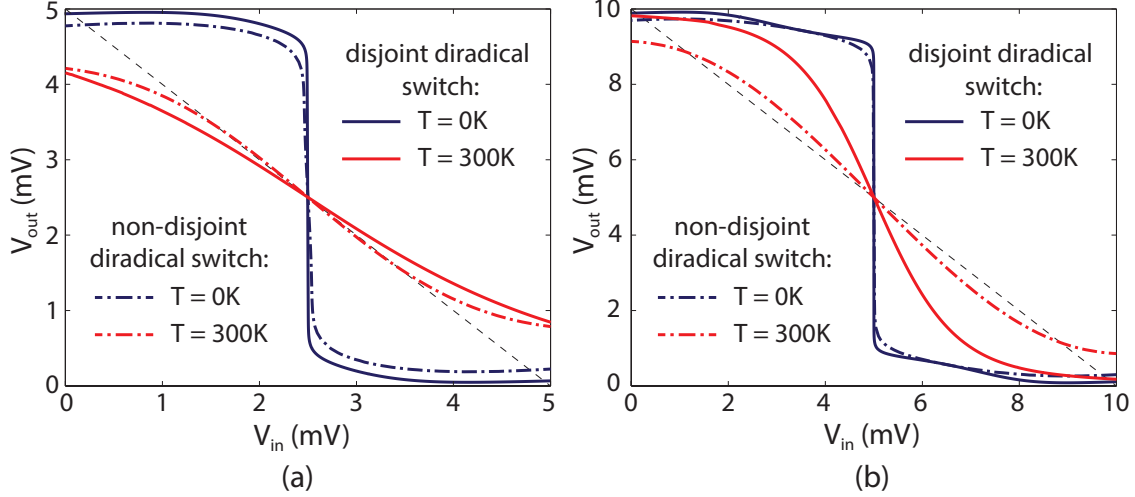


Figure 3: Numerically calculated voltage transfer characteristics for the quantum inverter based on \mathcal{PT} -symmetric interference transistors for room and zero temperature. Supply voltage is $V_0 = 5\text{mV}$ (a) and $V_0 = 10\text{mV}$ (b). The inverter operates at zero temperature better than at room temperature. Dashed black line shows the -1 slope for comparison.

The mean-square voltage uncertainty is $\Delta V_{therm} = \sqrt{kT/C}$, where C is the capacitance of the load, which is typically the gate capacitance of the next switch. Therefore, using several molecules in parallel in the single switch and, consequently, a bigger gate contact, will increase the capacitance C and lower the noise. But, on the other hand, the greater C is, the worse switching rate $\nu \sim (\tau)^{-1} = (RC)^{-1}$ can be achieved. Here the resistance R can be estimated from the current in the ‘on’ state (see Supplementary material): $R \approx \frac{\hbar}{e^2} \times \frac{2kT}{\pi\Gamma}$. Thus, restricting the minimum operating frequency ν_{min} , one can estimate the minimum allowed supply voltage, which we take to be 8 times the noise voltage uncertainty to provide an error probability at about 10^{-15} . [40] Finally we arrive at the following restriction:

$$V_0 > \sqrt{2 \frac{\hbar}{e^2} \times \frac{2(kT)^2}{\pi\Gamma}} \times \nu_{min}, \quad (20)$$

which for the room temperature and $\Gamma \approx 1\text{meV}$ gives $V_0 \gtrsim 10\text{mV} \times \sqrt{\nu_{min}}$, where ν_{min} is in GHz. Thus, sub- kT/e supply voltages seems to be possible up to $\nu \approx 7\text{GHz}$. More detailed analysis of noise impact on operation of quantum interference gates will be presented elsewhere, as well as consideration of technological parameter variation resulting in asymmetry of the inverter structure.

At the moment practical realization of high scale integration of quantum molecular gates is beyond the reach of modern technology. However continuous progress in self-assembling methods and, especially, development of atomic precision lithography could make almost inevitable the implementation of molecules as building blocks of ICs.

Appendix A: Electron occupation symmetry breaking

Real eigenvalues of the auxiliary Hamiltonian define the exact location of perfect transmission resonance and, being \mathcal{PT} -symmetric it can experience \mathcal{PT} -symmetry breaking, which results in resonance coalescence. This is accompanied by the symmetry breaking of electron occupation in the transmission maximum. The matrix of occupations per unit energy \hat{n} can be calculated within NEGF formalism: [33]

$$\hat{n} = \frac{1}{2\pi} \left[f_L(\omega) \hat{G}^r \hat{\Gamma}_L \hat{G}^a + f_R(\omega) \hat{G}^r \hat{\Gamma}_R \hat{G}^a \right], \quad (21)$$

where $f_{L,R}$ is the Fermi-Dirac distribution function in the left/right lead. Now suppose that symmetric and anti-symmetric states in the site basis are $|s\rangle = (s_1, s_2, \dots, s_N)^\top$ and $|a\rangle = (a_1, a_2, \dots, a_N)^\top$. Thus, neglecting the

contribution from distant energy levels, the occupations per unit energy of the i -th site (i.e. (i, i) diagonal element of the occupation matrix in the site basis) is following:

$$n_i = s_i^2 n_{ss} + a_i^2 n_{aa} + s_i a_i (n_{sa} + n_{as}). \quad (22)$$

Here $n_{s,s}$, $n_{s,a}$, $n_{a,s}$, and $n_{a,a}$ are elements of the occupation matrix in the basis of symmetric and anti-symmetric states. If the sites i and j are mapped into each other by the mirror reflection σ_{LR} (i.e. $j = \sigma_{LR}(i)$), then corresponding components of the symmetric and anti-symmetric states must be: $s_i = s_j$ and $a_i = -a_j$. Therefore, the difference between occupations of this sites is

$$n_i - n_{\sigma_{LR}(i)} = 2s_i a_i (n_{sa} + n_{as}) \propto n_{sa} + n_{as}. \quad (23)$$

This difference appears to be proportional to the sum of non-diagonal elements of the occupation matrix in the symmetric/anti-symmetric states basis. Utilizing Eq. (21) we can calculate this sum for our system:

$$n_i - n_{\sigma_{LR}(i)} \propto n_{sa} + n_{as} = \frac{\Gamma \gamma_s \gamma_s (f_L - f_R)}{\pi \left[4\Gamma^2 \gamma_a^4 + (\omega - \varepsilon - k_a \delta)^2 \right] \left[4\Gamma^2 \gamma_s^4 + (\omega - \varepsilon - k_s \delta)^2 \right]} \times |Q|, \quad (24)$$

where $|Q|$ is given by Eq. (9). Thus, it is obvious, that at perfect transmission resonances (real zeroes of Q) electron occupation is distributed symmetrically (with respect to σ_{LR} operation). Whereas, for energies, which correspond to transmission lower than 1, there is always asymmetric distribution of electrons. Therefore, coalescence of two perfect resonances into one non-perfect is always accompanied by a symmetry breaking of electron distribution, that was shown for linear systems in Ref. [28].

References

- [1] James K. Gimzewski and Christian Joachim. Nanoscale science of single molecules using local probes. *Science*, 283(5408):1683–1688, 1999.
- [2] Sriharsha V. Aradhya and Latha Venkataraman. Single-molecule junctions beyond electronic transport. *Nature Nanotechnology*, 8:399, Jun 2013. Review Article.
- [3] Juan Carlos Cuevas and Elke Scheer. *Molecular electronics: an introduction to theory and experiment*. World Scientific, 2010.
- [4] Arie Aviram and Mark A. Ratner. Molecular rectifiers. *Chemical Physics Letters*, 29(2):277 – 283, 1974.
- [5] A. K. Geim and K. S. Novoselov. The rise of graphene. *Nature Materials*, 6:183, Mar 2007.
- [6] Isaac Alc3n, Francesc Vi3es, Iberio de P. R. Moreira, and Stefan T. Bromley. Existence of multi-radical and closed-shell semiconducting states in post-graphene organic dirac materials. *Nature Communications*, 8(1):1957, 2017.
- [7] Christian Joachim and Mark A. Ratner. Molecular electronics: Some views on transport junctions and beyond. *Proceedings of the National Academy of Sciences*, 102(25):8801–8808, 2005.
- [8] Frank Schwierz. Graphene transistors. *Nature Nanotechnology*, 5:487, May 2010. Review Article.
- [9] Mervin Zhao, Yu Ye, Yimo Han, Yang Xia, Hanyu Zhu, Siqi Wang, Yuan Wang, David A. Muller, and Xiang Zhang. Large-scale chemical assembly of atomically thin transistors and circuits. *Nature Nanotechnology*, 11:954, Jul 2016. Article.
- [10] Shu-Jen Han, Jianshi Tang, Bharat Kumar, Abram Falk, Damon Farmer, George Tulevski, Keith Jenkins, Ali Afzali, Satoshi Oida, John Ott, James Hannon, and Wilfried Haensch. High-speed logic integrated circuits with solution-processed self-assembled carbon nanotubes. *Nature Nanotechnology*, 12:861, Jul 2017.
- [11] Qing Cao, Jerry Tersoff, Damon B. Farmer, Yu Zhu, and Shu-Jen Han. Carbon nanotube transistors scaled to a 40-nanometer footprint. *Science*, 356(6345):1369–1372, 2017.

- [12] Giuseppe Iannaccone, Francesco Bonaccorso, Luigi Colombo, and Gianluca Fiori. Quantum engineering of transistors based on 2d materials heterostructures. *Nature Nanotechnology*, 13(3):183–191, 2018.
- [13] Yuanbo Zhang, Tsung-Ta Tang, Caglar Girit, Zhao Hao, Michael C. Martin, Alex Zettl, Michael F. Crommie, Y. Ron Shen, and Feng Wang. Direct observation of a widely tunable bandgap in bilayer graphene. *Nature*, 459:820, Jun 2009.
- [14] Andrey E. Miroshnichenko, Sergej Flach, and Yuri S. Kivshar. Fano resonances in nanoscale structures. *Rev. Mod. Phys.*, 82:2257–2298, Aug 2010.
- [15] C. J. Lambert. Basic concepts of quantum interference and electron transport in single-molecule electronics. *Chem. Soc. Rev.*, 44:875–888, 2015.
- [16] Troels Markussen, Robert Stadler, and Kristian S. Thygesen. The relation between structure and quantum interference in single molecule junctions. *Nano Letters*, 10(10):4260–4265, Oct 2010.
- [17] Kim G. L. Pedersen, Mikkel Strange, Martin Leijnse, Per Hedegård, Gemma C. Solomon, and Jens Paaske. Quantum interference in off-resonant transport through single molecules. *Phys. Rev. B*, 90:125413, Sep 2014.
- [18] Yuta Tsuji, Roald Hoffmann, Ramis Movassagh, and Supriyo Datta. Quantum interference in polyenes. *The Journal of Chemical Physics*, 141(22):224311, 2014.
- [19] Gemma C Solomon. Interference effects in single-molecule transport. In *Handbook of Single-molecule Electronics*, pages 341–369. CRC Press LLC, 2015.
- [20] Davide Fracasso, Hennie Valkenier, Jan C. Hummelen, Gemma C. Solomon, and Ryan C. Chiechi. Evidence for quantum interference in sams of aryethynylene thiolates in tunneling junctions with eutectic ga-in (egain) top-contacts. *Journal of the American Chemical Society*, 133(24):9556–9563, Jun 2011.
- [21] Constant M. Guédon, Hennie Valkenier, Troels Markussen, Kristian S. Thygesen, Jan C. Hummelen, and Sense Jan van der Molen. Observation of quantum interference in molecular charge transport. *Nature Nanotechnology*, 7:305, Mar 2012.
- [22] H. Vazquez, R. Skouta, S. Schneebeli, M. Kamenetska, R. Breslow, L. Venkataraman, and M. S. Hybertsen. Probing the conductance superposition law in single-molecule circuits with parallel paths. *Nature Nanotechnology*, 7:663, Sep 2012.
- [23] Sriharsha V. Aradhya, Jeffrey S. Meisner, Markrete Krikorian, Seokhoon Ahn, Radha Parameswaran, Michael L. Steigerwald, Colin Nuckolls, and Latha Venkataraman. Dissecting contact mechanics from quantum interference in single-molecule junctions of stilbene derivatives. *Nano Letters*, 12(3):1643–1647, Mar 2012.
- [24] Charles A Stafford, David M Cardamone, and Sumit Mazumdar. The quantum interference effect transistor. *Nanotechnology*, 18(42):424014, 2007.
- [25] Ying Li, Jan A. Mol, Simon C. Benjamin, and G. Andrew D. Briggs. Interference-based molecular transistors. *Scientific Reports*, 6:33686, Sep 2016. Article.
- [26] A. A. Gorbatsevich and N. M. Shubin. Quantum analogs of cmos gates. *Usp. Fiz. Nauk*, accepted.
- [27] A.A. Gorbatsevich, M.N. Zhuravlev, and V.V. Kapaev. Collapse of resonances in semiconductor heterostructures as a transition with symmetry breaking in an open quantum system. *Journal of Experimental and Theoretical Physics*, 107(2):288–301, 2008.
- [28] A.A. Gorbatsevich and N.M. Shubin. Coalescence of resonances in dissipationless resonant tunneling structures and -symmetry breaking. *Annals of Physics*, 376:353 – 371, 2017.
- [29] A. A. Gorbatsevich and N. M. Shubin. Unified theory of resonances and bound states in the continuum in hermitian tight-binding models. *Phys. Rev. B*, 96:205441, Nov 2017.
- [30] Manabu Abe. Diradicals. *Chemical Reviews*, 113(9):7011–7088, Sep 2013.

- [31] Yuta Tsuji, Roald Hoffmann, Mikkel Strange, and Gemma C. Solomon. Close relation between quantum interference in molecular conductance and diradical existence. *Proceedings of the National Academy of Sciences*, 113(4):E413–E419, 2016.
- [32] Daijiro Nozaki, Andreas Lücke, and Wolf Gero Schmidt. Molecular orbital rule for quantum interference in weakly coupled dimers: Low-energy giant conductivity switching induced by orbital level crossing. *The Journal of Physical Chemistry Letters*, 8(4):727–732, Feb 2017.
- [33] S. Datta. *Electronic Transport in Mesoscopic Systems*. Cambridge Studies in Semiconductor Physics. Cambridge University Press, 1997.
- [34] D.A. Ryndyk, R. Gutiérrez, B Song, and G Cuniberti. Green function techniques in the treatment of quantum transport at the molecular scale. In *Energy Transfer Dynamics in Biomaterial Systems*, pages 213–335. Springer, Berlin, Heidelberg, 2009.
- [35] V. V. Sokolov and V. G. Zelevinsky. Collective dynamics of unstable quantum states. *Annals of Physics*, 216(2):323–350, 1992.
- [36] Carl M Bender. Making sense of non-hermitian hamiltonians. *Reports on Progress in Physics*, 70(6):947, 2007.
- [37] Akihiro Shimizu, Yasukazu Hirao, Kouzou Matsumoto, Hiroyuki Kurata, Takashi Kubo, Mikio Uruichi, and Kyuya Yakushi. Aromaticity and [small pi]-bond covalency: prominent intermolecular covalent bonding interaction of a kekule hydrocarbon with very significant singlet biradical character. *Chem. Commun.*, 48:5629–5631, 2012.
- [38] Weston Thatcher Borden and Ernest R. Davidson. Effects of electron repulsion in conjugated hydrocarbon diradicals. *Journal of the American Chemical Society*, 99(14):4587–4594, 1977.
- [39] W. Carl Lineberger and Weston Thatcher Borden. The synergy between qualitative theory, quantitative calculations, and direct experiments in understanding, calculating, and measuring the energy differences between the lowest singlet and triplet states of organic diradicals. *Phys. Chem. Chem. Phys.*, 13:11792–11813, 2011.
- [40] T. N. Theis and P. M. Solomon. In quest of the next switch: Prospects for greatly reduced power dissipation in a successor to the silicon field-effect transistor. *Proceedings of the IEEE*, 98(12):2005–2014, Dec 2010.
- [41] Adrian M. Ionescu and Heike Riel. Tunnel field-effect transistors as energy-efficient electronic switches. *Nature*, 479:329, Nov 2011.
- [42] A.P. Graham, G.S. Duesberg, W. Hoenlein, F. Kreupl, M. Liebau, R. Martin, B. Rajasekharan, W. Pamler, R. Seidel, W. Steinhögl, and E. Unger. How do carbon nanotubes fit into the semiconductor roadmap? *Applied Physics A*, 80(6):1141–1151, Mar 2005.
- [43] Lian-Mao Peng, Zhiyong Zhang, and Sheng Wang. Carbon nanotube electronics: recent advances. *Materials Today*, 17(9):433 – 442, 2014.
- [44] Ya.M. Blanter and M. Buttiker. Shot noise in mesoscopic conductors. *Physics Reports*, 336(1):1 – 166, 2000.